ONR TECHNICAL REPORT NO. 35

Project N 356-491

Contract: N00014-68-A-0131

EFFECT OF TEMPERATURE VARIATIONS ON MOLECULAR WEIGHT DISTRIBUTIONS - BATCH, CHAIN ADDITION POLYMERIZATIONS

by

Martin E. Sacks, Soo-Il Lee, and Joseph A. Biesenberger

Department of Chemistry and Chemical Engineering
Stevens Institute of Technology
Hoboken, New Jersey 07030

June, 1972

Accepted by

Chemical Engineering Sci.

Security Classification

DOCUMENT CONTROL DATA - R & D

Security classification of title, body of abstract and indexing annotation must be entered when the overall report is classified

ORIGINATING ACTIVITY (Corporate author) Stevens Institute of Technology Hoboken, New Jersey 07030	2a. REPORT SECURITY CLASSIFICATION 2b GROUP

1 REPORT TITLE

Effect of Temperature Variations on Molecular Weight Distributions - Batch, Chain Addition Polymerizations

4 DESCRIPTIVE NOTES (Type of report and, inclusive dates)

Technical Report

5 AUTHOR(S) (First name, middle initial, last name)

Martin E. Sacks, Soo-Il Lee, and Joseph A. Biesenberger

6 REPORT DATE	7a. TOTAL NO OF PAGES	7b. NO OF REFS
June 16, 1972	38	30

8a CONTRACT OR GRANT NO	9a. ORIGINATOR'S REPORT NUMBER(S)
N00014-68-A-0131	35
b. PROJECT NO NR 356-491	
c.	9b. OTHER REPORT NO(S) (Any other numbers that may be assigned this report)
d	

10 DISTRIBUTION STATEMENT

Qualified requesters may obtain copies of this report from the Department of Chemistry and Chemical Engineering, Stevens Institute of Technology, Hoboken, New Jersey 07030

11 SUPPLEMENTARY NOTES	12 SPONSORING MILITARY ACTIVITY
	Chemistry Program, Office of Naval Research, Washington, D.C.

13. ABSTRACT

The Maximum Principle was applied to determine the types of temperature variations that minimize and maximize the breadth of the molecular weight distribution (MWD) for chain addition polymerizations in batch reactors. It was found that the variations which minimize the breadth of the MWD keep the instantaneous number average chain length constant. The variations which maximize the breadth of the MWD are step changes in temperature resulting in bimodal distributions. Numerical and experimental examples of such variations are presented. MWDs with minimum and maximum breadths are compared to those that might be formed by temperature variations in real reactors. Under most conditions, temperature variations appear to have a much greater effect on MWD than residence time distributions and micromixing.

1

DD FORM 1 NOV 65 1473 (PAGE 1)

S/N 0101-807-6811

Security Classification

A-31409

ABSTRACT

The Maximum Principle was applied to determine the types of temperature variations that minimize and maximize the breadth of the molecular weight distribution (MWD) for chain addition polymerizations in batch reactors. It was found that the variations which minimize the breadth of the MWD keep the instantaneous number average chain length constant. The variations which maximize the breadth of the MWD are step changes in temperature resulting in bimodal distributions. Numerical and experimental examples of such variations are presented. MWD's with minimum and maximum breadths are compared to those that might be formed by temperature variations in real reactors. Under most conditions, temperature variations appear to have a much greater effect on MWD than residence time distributions and micromixing.

INTRODUCTION

Chain addition polymers are formed by the addition of monomer units, one at a time, to growing chains. These chains have life times which are much shorter than the half life of the monomer. Polymers produced by free radical mechanisms, such as polystyrene, low density polyethylene, poly-methyl methacrylate, etc., are examples of chain addition polymers.

Denbigh [1] first reported that polymers produced in commercial reactors would not generally have the same molecular weight distributions (MWD), and thus physical properties, as polymers produced in laboratory batch reactors. In particular he investigated the effect of residence time distributions (RTD) on MWD. Tadmor and Biesenberger [2] quantified the RTD effect and investigated the effect of micromixing as well. They found that the effects of RTD and micromixing on MWD were relatively small for chain addition polymers. These results were in agreement with the qualitative predictions of Denbigh, who reasoned that since the life times of growing chains were short compared to

the average residence time in a real reactor, RTD should have little effect on MWD. However, the important effects of temperature variations have not been studied in such detail. Chain addition polymerizations are highly exothermic, $\Delta H \doteq -15$ to -25 kcal/gmol. This coupled with the high viscosity and low thermal conductivity of polymer systems, makes heat transfer and thus temperature control difficult. In fact non-isothermal operation of bulk polymerization reactors is probably the rule rather than the exception.

The problem of determining the effect of temperature variations on the MWD can be attacked in two ways. The first is to model specific reaction systems. To some extent this has been done for tubular reactors [3], [4], [5]. The second way is to try to bound the effects of temperature, i.e., to determine what temperature variations minimize or maximize the breadth of the MWD. The second approach has been chosen for this study. This approach has the advantage that optimal control theory can be applied, and leads to generalized results.

Hoffman, et al. [6] and others [7,8,9], from a kinetic understanding of the polymerization process, proposed temperature and monomer or initiator addition policies which minimize the breadth of the MWD. These policies keep the instantaneous average chain length, $\bar{X}_{n,i}$, constant throughout the reaction. However, they are not always physically realizable because of constraints on the reactant concentrations and on the temperature. Ray and his co-workers [9] made numerical studies for a styrene polymerization model using optimal control theory. The best sub-optimal policies were found to be very close to the policies mentioned above.

In this paper the general nature of the temperature variations that minimize and maximize the breadth of the MWD will be deduced from the Maximum Principle. The polymerization model to be considered takes the gel effect into account emperically. Theoretical results are compared with experiments. Also, temperature policies which might exist in real reactors are discussed comparatively.

KINETIC MECHANISM

A typical free radical mechanism [10] with chemical initiation was chosen to describe the kinetics of the system. This mechanism consists of n^{th} order initiator decay, first order propogation with respect to monomer, and second order termination by combination and disproportionation. The absence of transfer reactions, and the principle of equal reactivity of growing chains were assumed. The mechanism can be represented by the following reactions:

$$I \xrightarrow{k_d} 2R \qquad (1)$$

$$R + M \xrightarrow{k_i} P_1 \qquad (2)$$

} Initiation; $R_i = 2fk_d h(I)$

$$P_x + M \xrightarrow{k_p} P_{x+1} \qquad (3)$$

Propogation

$$P_x + P_y \xrightarrow{k_{tc}} M_{x+y} \qquad (4)$$

$$P_x + P_y \xrightarrow{k_{td}} M_x + M_y \qquad (5)$$

} Termination

It is well known that many chain addition polymerizations are auto-catalytic [10]. This phenomenon has been termed the gel effect, and abundant experimental evidence indicates that it is due to a diffusion controlled termination. Theoretical [11] and emperical [12] relationships between k_t and solution viscosity have been proposed t account for the gel efrect. Since the viscosity of polymer solutions is primarily dependent on polymer concentration, as a first approximation, the overall termination constant was assumed to be an emperical, separable function of monomer conversion, m, and reciprocal temperature, $y = 1/R_gT$, to account for the gel effect.

$$k_t = k_{tc} + k_{td} = k_{to}(y) \cdot g^2(m) = A_t \exp(-E_t y) \cdot g^2(m) \qquad (6)$$

Assuming constant density and that primary radicals do not terminate, and applying the quasi steady state approximation [13], the following equations for

the conversion of monomer and initiator and for the first three moments of the MWD in a batch reactor can be derived.

$$\frac{dm}{dt} = \frac{d\xi_1}{dt} = k_1(y) \cdot h^{\frac{1}{2}}(1-c)\ (1-m)/g + 2ak_2(y) \cdot h(1-c) \tag{7}$$

$$\frac{dc}{dt} = k_2(y) \cdot h(1-c) \tag{8}$$

$$\frac{d\xi_0}{dt} = (2-\eta)\ ak_2(y) \cdot h(1-c) \tag{9}$$

$$\frac{d\xi_2}{dt} = 2(1+\eta)\ k_1(y) \cdot h^{\frac{1}{2}}(1-c)\ (1-m)/g + (2+\eta)k_3(y) \cdot (1-m)^2/g^2 + 2\eta ak_2(y) \cdot h(1-c) \tag{10}$$

Where $h(1-c)$ is any arbitrary function of initiator conversion. Details of the derivation of eqs. 7-10 are given in Appendix A. The number and weight average chain lengths are then given by:

$$\bar{X}_n = m/\xi_0 = m/[(2-\eta)ac] \tag{11}$$

$$\bar{X}_w = (\xi_2 + m)/m \tag{12}$$

The instantaneous number average chain length, i.e., the average length of dead chains being formed at any instant, is given by:

$$\bar{X}_{n,i} = \frac{dm}{d\xi_0} = \frac{1}{(2-\eta)a} \cdot \frac{k_1(y)}{k_2(y)} \cdot \frac{(1-m)}{h^{\frac{1}{2}}(1-c)g} + \frac{2}{(2-\eta)} \tag{13}$$

Eq. 13 shows that the gel effect, decreasing g, will result in an increase in the average chain length. For typical chain addition polymerizations $E_2 \doteq 30$ kcal/mol. while $E_1 \doteq 20$ kcal/mol. Thus k_1/k_2 has a negative activation energy, and $\bar{X}_{n,i}$ varies inversely with temperature. Finally, two modes of polymerization may be denoted from eq. 13 depending on the relative rates of conversion of monomer and initiator. In 'conventional' polymerization the rate of initiator conversion is slower than the rate of monomer conversion. $\bar{X}_{n,i}$ decreases with

time. In many 'conventional' polymerization systems the rate of initiator conversion is so low that, with negligible error, the initiator concentration may be assumed to be constant throughout the run. In 'dead end' polymerization [14] the rate of initiator conversion is faster than the rate of monomer conversion. $\bar{X}_{n,i}$ increases with time.

MINIMUM BREADTH

The objective of the problem is to determine what types of temperature variations result in the narrowest MWD's. The dispersion index:

$$D_n = \bar{X}_w/\bar{X}_n = 1 + (\sigma/\bar{X}_n)^2 \qquad (14)$$

will be used as a measure of the breadth of the MWD. To facilitate comparing results, D_n will be minimized at some predetermined monomer conversion, m*, and number average chain length, $\bar{X}_n$*. The temperature, and thus the reciprocal temperature, y, will be assumed to be physically constrained

$$T_* \leq T \leq T^*; \quad y^* \leq y \leq y_* \qquad (15)$$

These temperature bounds might be the temperature of the cooling water in the reactor jacket and the ceiling temperature of the polymer. Using eqs. 11 and 12, the problem can be formally stated as follows for the case of constant η: Find the temperature policy, y(t), subject to the constraints $y^* \leq y \leq y_*$, that minimizes ξ_2 (0) at a given m*(0) and c*(0).

For constant η the state of the system is described by eqs 7, 8, and 10. The Maximum Principle states that the optimal policy, y(t), which meets the problem objective, maximizes the Hamiltonian and makes it equal zero. Since we are considering only one control variable, y, these criteria can be formalized to yield:

$$H = 0$$

when y is unconstrained:

$$\frac{\partial H}{\partial y} = 0; \quad \frac{\partial^2 H}{\partial y^2} < 0; \quad y^* \leq y = y_s \leq y^* \qquad (16)$$

when y is at a constraint

$$\frac{\partial H}{\partial y} > 0 \quad ; \quad y = y_* \qquad (16)$$

$$\frac{\partial H}{\partial y} < 0 \quad ; \quad y = y^*$$

The Hamiltonian and adjoint variables are derived in Appendix B. Eq. 16 can then be applied to obtain the criteria for the optimal policy. Details of this procedure are also in Appendix B. When η and f are constant, the resulting criteria for the optimal policy are:

$$\bar{X}_{n,i} = \frac{k_1(1-m)}{(2-\eta)ak_2h^{\frac{1}{2}}g} + \frac{2}{(2-\eta)} < \frac{(\lambda_1-2-2\eta)}{(2+\eta)\ (2-\eta)} + \frac{2}{(2-\eta)} \quad ; \ y = y_* \qquad (17a)$$

$$\bar{X}_{n,i} = \frac{k_1\ (1-m)}{(2-\eta)\ ak_2h^{\frac{1}{2}}g} + \frac{2}{(2-\eta)} = \text{const} \quad ; \quad y^* \leq y = y_s \leq y_* \qquad (17b)$$

$$\bar{X}_{n,i} = \frac{k_1(1-m)}{(2-\eta)ak_2h^{\frac{1}{2}}g} + \frac{2}{(2-\eta)} > \frac{(\lambda_1-2-2\eta)}{(2+\eta)\ (2-\eta)} + \frac{2}{(2-\eta)} \quad ; \quad y = y^* \qquad (17c)$$

The stationary policy (17b), i.e., the policy that makes $\partial H/\partial y = 0$, is identical to the policy, postulated from a purely physical argument [6,7,8,9], which keeps $\bar{X}_{n,i}$ constant.

Physically, the optimal policy appears to minimize D_n by minimizing the change in the MWD caused by changing monomer and initiator concentrations during polymerization. Referring to eq. 13, $\bar{X}_{n,i}$ can be considered to be the product of a temperature dependent term, k_1/k_2, and a concentration dependent term, $\frac{(1-m)}{(2-\eta)a\ h^{\frac{1}{2}}g}$. The concentration dependent term is proportional to the isothermal $\bar{X}_{n,i}$, where the isothermal $\bar{X}_{n,i}$ is calculated at a temperature that results in the same m^* and $\bar{X}_n^*$ as the optimal policy. Three possible physical cases exist: 1) isothermal $\bar{X}_{n,i}$ decreases with time, 'conventional polymerization';

II) isothermal $\bar{X}_{n,i}$ increases with time, 'dead end polymerization' or very strong gel effect; and III) isothermal $\bar{X}_{n,i}$ decreases then increases with time, moderate gel effect. For each case three sub-cases exist depending on the initial temperature of the system. The initial temperature is in turn a function of the target m* and $\bar{X}_n$*, the initial concentration of reactants, and the initiator employed. The nine cases are summarized below:

I. Isothermal $\bar{X}_{n,i}$ decreases with time.

a. $y(0) = y_*$, Inequality 17a insures that the temperature remains equal to y_* throughout.

b. $y(0) = y_s$; Temperature decreases to keep $\bar{X}_{n,i}$ constant and may reach y_*, upon which the policy switches from y_s to y_*. Inequality 17a insures no further temperature change occurs.

c. $y(0) = y^*$; Temperature remains y^* until the inequality 17c comes to equality. When and if this occurs, the policy switches to y_s, a decreasing temperature policy. If y_s decreases to y_*, the policy switches to y_*. Inequality 17a insures that no further temperature change occurs.

II. Isothermal $\bar{X}_{n,i}$ increases with time.

a. $y(0) = y_*$; Temperature remains y_* until inequality 17a comes to equality. When and if this occurs, the policy switches to y_s, an increasing temperature policy to keep $\bar{X}_{n,i}$ constant. If y_s reaches y*, the policy switches to y*. Inequality 17c insures that no further temperature change occurs.

b. $y(0) = y_s$; Temperature increases to keep $\bar{X}_{n,i}$ constant. If y_s reaches y*, the policy switches to y*. Inequality 17c insures that no further temperature change occurs.

c. $y(0) = y^*$; Inequality 17c insures that the temperature remains y* throughout.

III. Isothermal $\bar{X}_{n,i}$ decreases then increases with time.

a. $y(0) = y^*$ Same as IIa

b. $y(0) = y_s$ On the decreasing portion of isothermal $\bar{X}_{n,i}$ (t)

the temperature decreases to keep $\bar{X}_{n,i}$ constant and may reach y_*, where the policy switches to y_*. On the increasing portion of isothermal $\bar{X}_{n,i}(t)$ the temperature increases to keep $\bar{X}_{n,i}$ constant, and may reach y^* where the policy switches to y^*. Inequality 17c insures that no further changes are possible.

c. $y(0) = y^*$. On the decreasing portion of isothermal $\bar{X}_{n,i}(t)$ inequality 17c may come to equality and the policy switches to y_s, a decreasing temperature policy and may reach y_*. If the switch from y^* to y_s occurs, the temperature increases on the increasing portion of isothermal $\bar{X}_{n,i}(t)$ and may reach y^* again. If the switch from y^* to y_s does not occur, the policy is y^* throughout.

Maximum Breadth

The objective of this problem is to determine the types of temperature variations that result in the broadest MWD's. The restrictions imposed in the minimum D_n case will again apply. The problem may be formally stated as follows: Find the temperature policy, $y(t)$, subject to the constraints $y^* \leq y \leq y_*$, that maximizes $\xi_2(0)$.

For constant η the state of the system is described by eqs. 7, 8 and 10. The Hamiltonian and adjoint variables are derived and eqs. 16 are applied to obtain the criteria for the optimal policy. Details of this procedure can be found in Appendix C. When f is constant, the resulting critera for the optimal policy are:

$$\bar{X}_{n,i} = \frac{\lambda_1(1-m)}{(2-\eta)ak_2h^{\frac{1}{2}}g} + \frac{2}{(2-\eta)} \leq -\frac{(\lambda_1+2+2\eta)}{(2+\eta)(2-\eta)} + \frac{2}{(2-\eta)} \quad ; y=y^* \qquad (18a)$$

$$\bar{X}_{n,i} = \frac{\lambda_1(1-m)}{(2-\eta)ak_2h^{\frac{1}{2}}g} + \frac{2}{(2-\eta)} \geq -\frac{(\lambda_1+2+2\eta)}{(2+\eta)(2-\eta)} + \frac{2}{(2-\eta)} \quad ; y=y_* \qquad (18b)$$

The stationary policy, $y^* \leq y_s \leq y_*$, cannot form part of the optimal path. The policy that maximizes D_n exists entirely on the bounding temperatures, y^* a

y_*, and therefore, the optimal temperature policy must consist of y^* or y_* or step changes between the two.

The number and direction of changes between y^* and y_* is determined by the sign of λ_1, the nature of the change in the isothermal $\bar{X}_{n,i}$ with time, and the initial temperature of the system.

If λ_1 is positive, 18 states that the temperature must be y_* for any initial conditions and target m^* and X_n^*. This is not the usual case since a policy of $y = y_*$ will not generally produce a polymer with the target conditions, m^* and $\bar{X}_n^*$. Therefore, λ_1 will generally be negative. When λ_1 is negative, six cases can be identified:

I. Isothermal $\bar{X}_{n,i}$ decreases with time:

a. $y(0) = y_*$. Inequality 18b may come to equality and the policy switches to y^*. Further switches are precluded by 18a.

b. $y(0) = y^*$. Policy is y^* throughout.

II. Isothermal $\bar{X}_{n,i}$ increases with time.

a. $y(0) = y_*$. Policy is y_* throughout.

b. $y(0) = y^*$. Inequality 18a may come to equality and the policy switches to y_*. Further switches are precluded by 18b.

III. Isothermal $\bar{X}_{n,i}$ decreases then increases with time.

a. $y(0) = y_*$. Inequality 18b may come to equality on decreasing segment of $\bar{X}_{n,i}$ vs. t and policy switches to y^*. If this occurs, inequality 18a may come to equality on the increasing segment of $\bar{X}_{n,i}$ vs. t, and the policy switches to y_*. Further switches are precluded by 18b.

b. $y(0) = y^*$. Inequality 18a may come to equality on the increasing segment of $\bar{X}_{n,i}$ vs. t and the policy switches to y_*. Further switches are precluded by 18b.

Since an isothermal policy of y^* or y_* will not generally reach a predetermined m^* and $\bar{X}_n^*$, most policies that maximize D_n will consist of one or at most two step changes in temperature, Cases Ia, IIb and IIIa&b. Unlike

the minimum D_n case, the physical stategy behind the optimal criteria is not evident from 18. However, this stategy will become evident when numerical examples are considered.

ISOTHERMAL $\bar{X}_{n,i}$

In the preceeding sections the general nature of the optimal policies that minimize and maximize the breadth of the MWD was found to depend on the variation of the isothermal $\bar{X}_{n,i}$ with time. This variation may be quantified by studying $d\bar{X}_{n,i}/dt$ at any fixed temperature level.

Differentiating eq. 13 with respect to time and substituting eq. 7 and 8 into the result, yields $d\bar{X}_{n,i}/dt$ at any fixed temperature level as a function of m and c. Dividing eq. 8 into eq. 7 after making the long chain approximation [10], neglecting the second term on the right hand side of eq. 7, and integrating, yields c as a function of m in an isothermal system. With this result, $d\bar{X}_{n,i}/dt$ can be rearranged to give the following criteria:

$$\frac{(k_2/2k_1)}{1 - \frac{k_2}{2k_1}\cdot W(m)} - \frac{g + (1-m)g'}{g^2} \begin{cases} < 0 \text{ ; Isothermal } \bar{X}_{n,i} \text{ decreases} \\ > 0 \text{ ; Isothermal } \bar{X}_{n,i} \text{ increases} \end{cases} \quad (19)$$

where $W(m) = \int_0^m g(m')dm'/(1-m')$ and $g' = dg/dm$. Eq. 19 was used to prepare maps of k_2/k_1 at various temperature levels versus conversion that show regions where isothermal $\bar{X}_{n,i}$ increases and decreases. Maps for styrene, methyl methacrylate and for polymerization without the gel effect are shown on Figure 1.

CONTROLLABILITY

In the preceeding sections it was tacitly assumed that it was possible to reach the target conditions, m* and $\bar{X}_n$*, by some constrained temperature policy, $T_* \leq T \leq T^*$. It may not always be possible to do this, however, because of insufficient reactant concentrations or temperature constraints that are

too narrow. Such systems are not controllable.

The limits of controllabiliby are given by:

$$\bar{X}_n\Big|_{\substack{m=m^* \\ T=T^*}} \leq \bar{X}_n^* \leq \bar{X}_n\Big|_{\substack{m=m^* \\ T=T_*}} \tag{20}$$

$$\frac{f l_o^n}{M_o} \leq a \geqslant \frac{m^*}{(2-\eta)} \cdot \frac{1}{\bar{X}_n^*} \tag{21}$$

NUMERICAL EXAMPLES

Two vinyl polymerization systems, poly-styrene and poly-methyl methacrylate initiated by aso-bis-iso-butrylnitrile (AIBN), were chosen, and numerical examples of optimal temperature policies were calculated.

The initiator decay is first order, $h(1-c) = 1-c$.

The kinetic data that were used are summerized in Table 1.

Kinetic constants for styrene were taken from Hamielec, et al. [15]. The gel effect function, g, was obtained from the data of Tobolsky, et al. [16] and Nishimura [17]. Bevington, et al. [18] showed that termination for polystyrene occurs exclusively by combination, $\eta=1$. Kinetic constants for methyl methacrylate were chosen by comparing the individual rate constants determined by various workers [18,19,20,21,22] to the apparent rate constant, k_t/k_p^2, obtained by Bevington, et al. [23] and by Baysal and Tobolsky [24]. On this basis the individual rate constants used by King and Skaates [25] were chosen. The gel effect function was obtained from the data of Hayden and Melville [19]. The data of Bevington, et al. [18] and of Obrian and Gornick [26] for methyl methacrylate show that η is a function of temperature. However, the primary mode at temperatures of interest appears to be disproportionation, $\eta=0$, and, therefore, termination was assumed to occur exclusively by this mechanism.

Optimal policies were calculated on a PDP-10 digital computer. The calculation procedure used was as follows:

1. Guess $\lambda_1(0)$

2. Numerically integrate eq. 7, 8, 10 and B-2 using a 3-point Runge-Kutta algorithm. At each increment solve eq. 17 or 18 to determine the optimal reciprocal temperature, y.

3. At m=m* compare $\bar{X}_n$ to the desired value, $\bar{X}_n$*, defining the error as $(\bar{X}_n^* - \bar{X}_n)^2$.

4. Use a Fibonacci search technique [27] to adjust the value of $\lambda_1(0)$.

5. Repeat 2-4 until the error is less than some predetermined value.

It was found convenient to use a similar procedure to determine the isothermal policy yielding the same m* and $\bar{X}_n$* as the optimal policy. The initial temperature of the system was guessed and adjusted to reduce the error. Also the policy consisting of a step increase from T_* to T* which yields the same m* and $\bar{X}_n$* as the optimal policies was calculated for comparison. This policy would be the most extreme temperature rise possible.

The results of five such calculations are summerized in Table II. Reaction conditions, conversions, $\bar{X}_n$ and the dispersion indicies for the policies that maximize D_n, minimize D_n and reach m* and $\bar{X}_n$* isothermally and with a step rise from T_* to T* are presented. Runs with the suffix 'A' were calculated without the gel effect. The following conclusions can be drawn from Table II:

1. The minimum D_n is significantly less than the isothermal D_n when a strong gel effect is present (exs. 4 and 5) or when a moderate gel effect and dead end conditions exist simultaneously (ex. 2). Under these conditions, isothermal $\bar{X}_{n,i}$ varies significantly over the course of the reaction. Under conventional conditions, minimum and isothermal D_n's are about the same.

2. The maximum D_n is significantly greater than the isothermal D_n for all the examples in Table II. The gel effect (compare examples with the suffix 'A' to those without it) and dead end conditions (compare ex. 2 to ex. 1 and ex. 5 to ex. 4) increase the maximum D_n.

3. The step rise D_n is significantly greater than the isothermal D_n for all the examples except ex. 5. The gel effect and dead end conditions generally decrease the step rise D_n.

4. The maximum D_n is significantly greater than the D_n from a segregated continuous stirred tank reactor (SCSTR). Tadmor and Biesenberger [2] found that the SCSTR gives the broadest MWD of any isothermal reactor for chain addition polymerizations. Thus, the maximum effects of temperature variations on MWD's are much greater than the maximum effects of residence time distributions or micromixing.

5. Maximum D_n's resulting from thermal effects alone are in the range of those reported [28] for low density polyethylene. Therefore, non-isothermal reactor conditions may be at least partially responsible for these high dispersities.

The temperature policies and resulting instantaneous and cumulative number and weight average chain lengths are plotted versus monomer conversion for examples 1, 2 and 3 on Figures 2, 3, and 4, respectively. Examples of the three possible types of behavior of isothermal $\bar{X}_{n,i}$ are shown on these figures.

Figure 2 shows the optimal policies for the case where the isothermal $\bar{X}_{n,i}$ decreases then increases with time. The temperature policy that minimizes D_n decreases then increases to keep $\bar{X}_{n,i}$ constant. The temperature policy that maximizes D_n is a step increase then a step decrease in temperature from $T_* = 40^oC$ to $T^* = 120^oC$ to T_*. This policy results in a bimodal distribution with one mode formed at 40^oC, $\bar{X}_{n,i} \doteq 850$, and the other formed at 120^oC, $\bar{X}_{n,i} \doteq 40$. The cumulative number average chain length is determined primarily by the high temperature, low molecular weight mode, while the cumulative weight average chain length is determined primarily by the low temperature, high molecular weight mode.

Figure 3 shows the optimal policies for the case where the isothermal $\bar{X}_{n,i}$

increases with time. The minimum D_n policy is one of increasing temperature which keeps $\bar{X}_{n,i}$ constant. The maximum D_n policy is a step decrease in temperature which again results in a bimodal distribution.

Figure 4 shows the optimal policies for the case where the isothermal $\bar{X}_{n,i}$ decreases with conversion. The minimum D_n policy is one of decreasing temperature which keeps $\bar{X}_{n,i}$ constant. The maximum D_n policy is a step increase in temperature which results in a bimodal distribution.

The bimodal nature of the distributions produced by the maximum D_n policy and by the step increase policy of example 2 are shown in Figure 5. MWD's produced by the isothermal and minimum D_n policies are also plotted on Figure 5.

The physical strategy behind the maximum D_n policy is elucidated by the numerical examples. D_n is a measure of the standard deviation or, to use a physical analogy, the moment of inertia of the MWD. The moment of inertia of the MWD will be maximized if all the polymer molecules lie at the extremes of the distribution just as the moment of inertia of a body is maximized if all its weight is concentrated at its ends. Therefore, the maximum D_n policy seeks to form a bimodal distribution with the widest possible separation between the modes. The physical rational behind the direction and number of step changes can be seen with the aid of Figure 6. Inspection of Figure 6 shows that step changes in other than the directions indicated by the solid lines result in less than maximum D_n's. The up-slopes of the isothermal $\bar{X}_{n,i}$ curves for Cases II and III on Figure 6 increase with increasing gel or dead end effects. Therefore, the separation of the modes, when optimal directioned changes are made, increases, and the ratio of maximum D_n to isothermal D_n increases. Conversely, non-optimal directioned changes increase the overlap of the modes and result in a decrease in the ratic of step rise to isothermal D_n's.

EXPERIMENTAL EXAMPLES

Styrene initiated by AIBN was polymerized using step change temperature policies. The resulting polymers were analyzed by Gel Permeation Chromatography (GPC) to see if bimodal distributions could indeed be formed by temperature variations alone.

Apparatus and Procedure

Styrene (Eastman #1465 stabilized with tert-buty pyrocatechol) was purified by washing with 2% KOH followed by distilled water. The styrene was then dried over anhydrous calcium chloride, distilled under vacuum, and stored on ice for not more than 1 hour. Solutions of cold styrene and AIBN (Eastman #6400 2,2' Azobis (2-methylpropionitrile)) were made up gravimetrically. Reaction tubes (Ver Tis drying ampoule, 25 ml) were filled with about 10 ml of the cold solution. The tubes were degassed under 5 mm vacuum by 4 cycles of freezing and thawing and sealed. Tubes were stored frozen until used.

Prior to making a run, the tubes were allowed to thaw. During a run, the tubes were agitated by clamping them to mechanical stirrers immersed in a constant ($\pm$0.2°C) temperature bath. To approximate step temperature changes 2 baths at different temperatures were used, and the tubes were quickly transfered from one bath to the other.

At the end of a run tubes were quenched by plunging them into ice. The tubes were then opened, the polymer-monomer solutions were weighed, dissolved in 2 volumes of benzene and the polymer was precipitated in excess chilled methanol. After standing in a refrigerator overnight, the polymer was separated by centrifuging at 20,000 RPM for 1 hour. Conversions were determined gravimetrically.

The recovered polymer was then analyzed using a Waters Model 200 GPC. Five Styrogel (Waters Associates) packed columns with nominal pore diameters of $7X10^5$, $3X10^4$, 10^4, 250 and 10^3 Å were used. The ODCB plate count for the 5 column system was 650 plates/ft. The GPC was calibrated using mono-disperse styrene

EXPERIMENTAL EXAMPLES

Styrene initiated by AIBN was polymerized using step change temperature policies. The resulting polymers were analyzed by Gel Permeation Chromatography (GPC) to see if bimodal distributions could indeed be formed by temperature variations alone.

Apparatus and Procedure

Styrene (Eastman #1465 stabilized with tert-buty pyrocatechol) was purified by washing with 2% KOH followed by distilled water. The styrene was then dried over anhydrous calcium chloride, distilled under vacuum, and stored on ice for not more than 1 hour. Solutions of cold styrene and AIBN (Eastman #6400 2,2' Azobis (2-methylpropionitrile)) were made up gravimetrically. Reaction tubes (Ver Tis drying ampoule, 25 ml) were filled with about 10 ml of the cold solution. The tubes were degassed under 5 mm vacuum by 4 cycles of freezing and thawing and sealed. Tubes were stored frozen until used.

Prior to making a run, the tubes were allowed to thaw. During a run, the tubes were agitated by clamping them to mechanical stirrers immersed in a constant ($\pm$0.2°C) temperature bath. To approximate step temperature changes 2 baths at different temperatures were used, and the tubes were quickly transfered from one bath to the other.

At the end of a run tubes were quenched by plunging them into ice. The tubes were then opened, the polymer-monomer solutions were weighed, dissolved in 2 volumes of benzene and the polymer was precipitated in excess chilled methanol. After standing in a refrigerator overnight, the polymer was separated by centrifuging at 20,000 RPM for 1 hour. Conversions were determined gravimetrically.

The recovered polymer was then analyzed using a Waters Model 200 GPC. Five Styrogel (Waters Associates) packed columns with nominal pore diameters of $7X10^5$, $3X10^4$, 10^4, 250 and 10^3 Å were used. The ODCB plate count for the 5 column system was 650 plates/ft. The GPC was calibrated using mono-disperse styrene

samples (Pressure Chemicals).

Results

Initially four isothermal runs were made to test the validity of the kinetic model and constants (Table I). The agreement was quite good so two sets of maximum D_n and isothermal runs, each set having the same m^* and $\bar{X}_n^*$, were made. One set was made under conditions requiring a step decrease in temperature and the other under conditions requiring a step increase in temperature. The results of these 8 runs are summarized in Table III.

The initial isothermal runs are runs 1 to 4. Runs 5 and 6 form one set of isothermal and maximum D_n runs with $m^* \doteq 0.25$ and $\bar{X}_n^* \doteq 550$. The conditions were dead end, so the maximum D_n policy is a step decrease ($T_* = 40^oC$, $T_* = 100^oC$). Runs 7 and 8 form the second set with $m^* \doteq 0.33$ and $X_n^* \doteq 150$. The conditions were conventional so the maximum D_n policy is a step increase.

For all 8 runs the agreement between the experimental and calculated conversions is excellent. The values agree within about 10% for all runs except runs 2 and 6, where the agreement is within about 20%.

Agreement between the experimental (determined by GPC and reported uncorrected for diffusional effects) and the calculated weight average chain lengths is not as good. Except for run 6, the calculated values average about 25% lower than the experimental values. Part of this is due to diffusional effects in the GPC columns. Experimentally determined average chain lengths are compared to the values reported by the National Bureau of Standards for their sample NBS-706 in Table III. Their value for $\bar{X}_w$ is about 10% lower than the experimentally determined value. The method of Ishige, et al. [29] to correct chromatograms for diffusional effects was tried. It was not successful, probably due to skewing in our GPC. Nevertheless, the agreement between uncorrected experimental and calculated chain lengths is sufficiently good to show that the maximum D_n policy results in a significant increase in D_n compared to the isothermal policies.

Normalized chromatograms for runs 5 and 6, and 7 and 8 are compared to each other and to theoretical chromatograms obtained from the calculated MWD's for these runs on Figure 7. Runs 5 and 7, isothermal, are unimodal, while runs 6 and 8, maximum D_n, are bi-modal, as predicted.

To summarize, distributions that were produced under non-isothermal conditions predicted to maximize D_n had dispersion indicies that were approximatly 3 times the maximum D_n that would be predicted [2] for an isothermal system.

IDEALIZED BATCH REACTORS

Having bounded the problem by considering temperature variations that minimize and maximize the breadth of the MWD, it is fair to ask what effect actual temperature variations that might occur in polymerization reactors would have on the breadth of the MWD. Would actual temperature variations result in D_n's near those predicted by maximum D_n policies or would they be closer to those predicted for isothermal systems? As a first approximation to answering this question, temperature variations in an idealized batch reactor were considered.

The idealized reactor is assumed to be a batch reactor with a heat transfer surface (jacket or coil). The reactor is well agitated so it is homogeneous with respect to composition and temperature. The overall heat transfer coefficient of the jacket or coil is assumed to be constant, independent of conversion or temperature. With these assumptions the heat balance on the reactor can be written as:

$$\frac{d\phi}{dt} = -\alpha\phi + \frac{N_{ad}}{(T_f - T_o)} \frac{dm}{dt} \qquad (22)$$

where α is the reactor diffusivity and N_{ad} is the adiabatic temperature rise for the polymer. Eq. 22 was solved numerically in conjunction with eqs. 7, 8, and 10 to determine the effect of naturally occuring temperature variations on MWD.

Some temperature profiles for the bulk polymerization of styrene initiated by AIBN (I_o = 0.348 mol./l.) with h(1-c) = 1-c and an initial and coolant temperature of 40°C, and a final temperature of 120°C are shown on Figure 8. α was varied from 0 to 0.01 to simulate temperature profiles from adiabatic to isothermal. Dispersion indices for ϕ = 1 or m = 0.9 are shown on the curves. For this case and others not shown, the highest D_n is not produced by the adiabatic temperature rise (α = 0). Conditions under which some long chains are initially produced at low temperatures, followed by a rapid temperature rise producing short chains, results in the highest D_n's.

The broadest MWD formed under the conditions of Figure 8 (α = 0.00025) is compared to the MWD's for the maximum and minimum D_n policies resulting in the same m*, 0.261, and $\bar{X}_n$*, 71, on Figure 9. The dispersion indices for the three cases are 3.45, 7.61 and 1.49, respectively. The polymerization conditions are conventional. The isothermal case has approximately the same MWD and D_n as the minimum D_n case. The temperature variations in an idealized batch reactor resulted in a D_n about double that of the isothermal case and about half that of the maximum D_n case. Therefore, conditions exist where the D_n produced by naturally occurring temperature variations approaches the maximum D_n. In general such conditions will lead to conventional polymerization where the isothermal $\bar{X}_{n,I}$ decreases with time. For conventional polymerizations the maximum D_n policy is a step increase in temperature, and this is simulated, to some extent, by the temperature rise in the idealized batch reactor. On the other hand, the minimum D_n policy for dead end polymerizations or polymerizations with a strong gel effect is one of increasing temperature, and in these cases the temperature rise in the idealized batch reactor may not yield a polymer with a broader MWD than the isothermal case.

In real reactors another factor must be considered, non-homogeneity. Gradients and hot spots in batch and continuous stirred tank reactors, and radial

as well as axial gradients in tubular reactors should result in much broader MWD's than those predicted by the idealized model used here [3]. Therefore, the maximum D_n policy may be a valid upper limit for the breadth of the MWD from real reactors.

CONCLUSIONS

1. The temperature variations that minimize the breadth of the MWD keep instantaneous number average chain length constant. Such variations keep the MWD distribution from changing due to changes in monomer and initiator concentrations. Such variations are decreasing temperatures under conventional conditions where the isothermal $\overline{X}_{n,i}$ decreases with time, and increasing temperatures under strong gel or dead end conditions where the isothermal $\overline{X}_{n,i}$ increases with time.

2. The temperature variations that maximize the breadth of the MWD are step changes in temperature between the minimum and maximum allowable temperatures in the system. Such variations produce a bimodal distribution with the maximum separation between modes. For conventional polymerization, isothermal $\overline{X}_{n,i}$ decreases with time, the optimal variation is one step increase in temperature. For dead end polymerization, isothermal $\overline{X}_{n,i}$ increases with time, the optimal variation is one step decrease in temperature. For polymerization with a gel effect, isothermal $\overline{X}_{n,i}$ decreases then increases with time, the optimal variation is a step increase followed by a step decrease in temperature.

3. Temperature variations have a much greater effect on the breadth of MWD's for chain addition polymerizations than residence time distributions or micomixing.

4. Rising temperatures which may occur in real reactors can lead to a significant increase in the breadth of the MWD compared to isothermal operation. In general this effect will be greater for conventional polymerizations than for dead end polymerizations or polymerizations with a strong gel effect.

NOTATION

a	initial reactant ration, fI_o^n/M_o
A	heat transfer area
A_d, A_p, A_t	frequency factor for initiator decomposition, propogation, and termination, respectively.
c	initiator conversion, $(1 - I/I_o)$
c^*	target initiator conversion
c_v	heat capacity
D_n	dispersion index, $\overline{X}_w/\overline{X}_n$
E_d, E_p, E_t	activation energies for initiator decomposition, propogation, and termination.
f	initiator efficiency
F	moment generating function defined by A-7
g	gel effect function, $g(m) = (k_t/k_{to})^{\frac{1}{2}}$
G	moment generating function defined by eq. A-7
ΔH	heat of polymerization
H	Hamiltonian, $\sum_i \lambda_i \, (dX_i/dt)$
h	$(1-c)^n$
I	initiator concentration
I_o	initial initiator concentration
k_d, k_p	kinetic constants for initiator decomposition and for propogation, respectively
k_t	termination constant, $(k_{tc} + k_{td}) = k_{to}(y) \cdot g^2(m)$
k_1	$k_p(2fI_o^n k_d/k_{to})^{\frac{1}{2}} = A_1 \exp(-E_1 y)$
k_2	$I_o^{n-1} k_d = A_2 \exp(-E_2 y)$
k_3	$M_o k_p^2/k_t = A_3 \exp(-E_3 y)$
m	monomer conversion, $(1-M/M_o)$
m^*	target monomer conversion
M	monomer concentration
M_o	initial monomer concentration

M_x	concentration of dead polymer of length x
N_{ad}	adiabatic temperature rise, $-\Delta H/(MW \cdot c_v)$
P_x	concentration of growing chains of length x
q_n	n^{th} moment of the dead polymer distribution, defined by eq. A-8.
R	concentration of primary radicals
R_g	gas constant
t	time
T	absolute temperature
T_f	final temperature
T_o	initial temperature, coolant temperature
V	Reactor volume
U	Overall heat transfer coefficient
$\bar{x}$	state vector with components x_i
$\bar{X}_n$	number average chain length
$\bar{X}_n^*$	target number average chain length
$\bar{X}_{n,i}$	instantaneous number average chain length, $dm/d\xi_o$
$\bar{X}_w$	weight average chain length
y	reciprocal temperature, $1/R_g T$
y_*	maximum y, corresponds to physically constrained minimum temperature. T_*.
y^*	minimum y, corresponds to physically constrained maximum temperature, T^*
y_s	stationary temperature policy. Solution to $\partial H/\partial y = 0$
z_n	n^{th} moment of the living polymer distribution, defined by eq. A-8

GREEK LETTERS

α	reactor diffusivity, $(UA/V\rho\ c_v)$
η	ratio of k_{tc}/k_t
λ_i	adjoint variable, $-\partial H/\partial X_i$

ϕ dimensionless temperature, $(T-T_o)/(T_f-T_o)$

ρ density

σ standard deviation

ξ_n dimensionless n^{th} moment of the dead polymer distribution, q_n/M_o

REFERENCES

[1] Denbigh K.G., J. Appl. Chem. 1951 1 227

[2] Tadmor Z, Biesenberger J.A. Indl Engng Chem. Fund 1966 5 336.

[3] Cintron R., Mostello R.A., Biesenberger J.A., Can J. Chem. Engng 1968 46 434.

[4] Cintron R, "Ph.D Thesis" Stevens Inst., Hoboken, 1971.

[5] Lynn S., Huff J.E., AIChE J1 1971 17 475.

[6] Hoffman R., Schreiber S., Rosen G., Indl Engng Chem 1964 56 (5) 51.

[7] Tadmor Z., Biesenberger J.A., J. Polymer Sci Pt. B 1965 3 753.

[8] Lee S-I, Imoto T., "Polymerization Engineering" Nikkankogyo Tokyo 1970.

[9] Hicks J., Mohan A., Ray W.H., Can J Chem Engng 1969 47 590.

[10] Bamford C.H., Barb W.G., Jenkins A.D., Onyon P.F., "The Kinetics of Vinyl Polymerization," Butterworths London 1958.

[11] Benson S.W., North A.M., J Am Chem Soc 1962 84 935.

[12] Hui A.W., Hamielec A.E., J Polymer Sci PtC 1968 No. 25 167.

[13] Biesenberger J.A., Capinpin R., to be published in J Appl Polymer Sci.

[14] Tobolsky A. V., J Am Chem Soc 1958 80 5927.

[15] Duerksen J.H., Hamielec A.E., Hodgins J.W., AIChE J1 1967 13 1081.

[16] Tobolsky A.V., Rogers C.E., Brickman J.W., J Am Chem Soc 1960 82 1277.

[17] Nishimura N, J Macromol Chem 1966 1 257.

[18] Bevington J.C., Melville H.W., Taylor R.P., J Polymer Sci 1954 14 463.

[19] Hayden P., Melville H., J Polymer Sci 1960 43 201.

[20] Mackay M.H., Melville H.W., Trans Faraday Soc 1949 45 323.

[21] Matheson M.S., Auer E.E., Bevilacqua E.B., Hart E.J. J Am Chem Soc 1947 71 497.

[22] Yokota K., Kani M., Ishii Y. J Polymer Sci Pt A-1 1965 6 1325.

[23] Bevington J.C., Melville H.W., Taylor R.P., J Polymer Sci 1954 12 449.

[24] Baysal B., Tobolsky A.V., J Polymer Sci 1952 8 529.

[25] King P.E., Skaates J.M., Indl Engng Chem Process Des Develop 1969 8 114.

[26] Obrian J.L., Gornick F., J Am Chem Soc 1955 77 4757.

[27] Denn M., "Optimization by Variational Methods" McGraw-Hill, New York 1969.

[28] Beasley J.K., J Am Chem Soc 1953 75 6123.

[29] Ishige T., Lee S-I, Hamielec A.E., J Appl. Polymer Sci 1971 15 1607.

[30] Ray W.H., Can J Chem Engng 1967 45 356.

Acknowledgement

This work was supported in part by the Office of Naval Research. The authors would also like to thank the Plastics Institute of America for its financial support.

APPENDIX A. DERIVATION OF STATE EQUATIONS

With the assumption of constant density and that primary radicals do not terminate differential mass balances for a batch reactor can be written from reactions 1-5.

$$\frac{dI}{dt} = -k_d h\ (I) \qquad \text{(A-1)}$$

$$\frac{dM}{dt} = -k_p M \sum_{n=1}^{\infty} P_n - k_i MR \qquad \text{(A-2)}$$

$$\frac{dR}{dt} = 2fk_d h(I) - k_i MR \qquad \text{(A-3)}$$

$$\frac{dP_1}{dt} = k_i MR - k_p MP_1 - (k_{tc} + k_{td})\ P_1 \sum_{n=i}^{\infty} P_n \qquad \text{(A-4)}$$

$$\frac{dP_x}{dt} = k_p M\ (P_{x-1} - P_x) - (k_{tc} + k_{td})\ P_x \sum_{n=1}^{\infty} P_n \qquad \text{(A-5)}$$

$$\frac{dM_x}{dt} = \tfrac{1}{2}k_{tc} \sum_{i=1}^{x-i} P_i P_{x-i} + k_{td} P_x \sum_{n=1}^{\infty} P_n \qquad \text{(A-6)}$$

The moments of the MWD are derived by means of moment generating functions [30].

$$G(r,x) = \sum_{x=1}^{\infty} r^x P_x \ ; \qquad F(r,x) = \sum_{x=1}^{\infty} r^x M_x \qquad \text{(A-7)}$$

from which the moments of the living and dead chain distributions can be obtained by differentiation

$$z_n = \frac{\partial^n G(1,x)}{\partial r^n} \ ; \ q_n = \frac{\partial^n F(1,x)}{\partial r^n} \qquad \text{(A-8)}$$

G and F are derived by summing r^x times eq. A-5 and r^x times eq. A-6, respectively.

$$\frac{dG}{dt} = k_i MR - k_p M \sum_{x=1}^{\infty} r^x P_x + k_p M \sum_{x=1}^{\infty} r^{x+1} P_x$$

$$-(k_{tc} + k_{td}) \sum_{x=1}^{\infty} r^x P_x \sum_{x=1}^{\infty} P'_x \qquad \text{(A-9)}$$

$$\frac{dF}{dt} = k_{td} \sum_{x=1}^{\infty} r^x P_x \sum_{n=1}^{\infty} P_n + (k_{tc}/2) \sum_{x=1}^{\infty} r^x \sum_{i=1}^{x-1} P_i P_{x-i} \qquad \text{(A-10)}$$

The resulting moment balances are:

$$\frac{dz_o}{dt} = k_i MR - (k_{tc} + k_{td}) z_o^2 \qquad \text{(A-11)}$$

$$\frac{dz_1}{dt} = k_i MR + k_p M z_o - (k_{tc} + k_{td}) z_o z_1 \qquad \text{(A-12)}$$

$$\frac{dz_2}{dt} = 2k_p M z_1 - (k_{tc} + k_{td}) z_o z_2 \qquad \text{(A-13)}$$

$$\frac{dq_o}{dt} = (k_{td} + \frac{k_{tc}}{2}) z_o^2 \qquad \text{(A-14)}$$

$$\frac{dq_1}{dt} = (k_{tc} + k_{td}) z_o z_1 \qquad \text{(A-15)}$$

$$\frac{dq_2}{dt} = (k_{tc} + k_{td}) z_o z_2 + k_{tc} z_1^2 \qquad \text{(A-16)}$$

Eqs. A-11 to -16 were obtained with the aid of the following identities:

$$\sum_{x=1}^{\infty} P_x \sum_{n=1}^{\infty} P_n = \sum_{x=1}^{\infty} \sum_{i=1}^{x-1} P_i P_{x-i}$$

$$\sum_{x=1}^{\infty} xP_x \sum_{n=1}^{\infty} P_n = \tfrac{1}{2} \sum_{x=1}^{\infty} x \sum_{i=1}^{x-1} P_i P_{x-i} \qquad \text{(A-17)}$$

$$\tfrac{1}{2} \sum_{x=1}^{\infty} (x^2-x) \sum_{i=1}^{x-1} P_i P_{x-i} = \left(\sum_{x=1}^{\infty} xP_x \right)^2 + \sum_{x=1}^{\infty} P_x \sum_{n=1}^{\infty} (n^2-n) P_n$$

Invoking the quasi steady state approximation (QSSA), which assumes that the left hand sides of eqs. A-3,4 and 5 are small compared to the individual terms on the right, allows us to set dP_x/dt and dR/dt equal to zero. Applying

the QSSA to A-3, -11 to -13 yields:

$$z_o = \left(\frac{2fk_d h(1)}{k_{tc}+k_{td}}\right)^{\frac{1}{2}} \quad ; \quad z_1 = z_o + \frac{k_p M}{k_{tc}+k_{td}} \quad ; \quad z_2 = \frac{2k_p M z_1}{(k_{tc}+k_{td})z_o} \qquad (A\text{-}19)$$

Substitution of A-18 and the deffinitions of m, c, η, the dimensionless moments, ξ_i, and the lumped kinetic constants, k_1, k_2 and k_3, in A-14 to -16 yields the state eqs. 10-13.

APPENDIX B. DERIVATION OF CRITERIA FOR THE MINIMUM D_η POLICY

When η is constant the state of the system is described by equations 7,8 and 10. The optimal policy makes the Hamiltonian a maximum and zero. The Hamiltonian is given by:

$$H = 0 = \lambda_1 \left[k_1 h^{\frac{1}{2}}(1-c)\frac{(1-m)}{g} + 2ak_2 h(1-c)\right] + \lambda_2 k_2 h(1-c) + \lambda_3 \left[(2+\eta)k_3 \frac{(1-m)^2}{g^2} + 2(1+\eta)k_1 h^{\frac{1}{2}}(1-c)\frac{(1-m)}{g} + 2\eta a k_2 h(1-c)\right] \qquad (B\text{-}1)$$

When f is constant, the adjoint variables ($\lambda_i = -\partial H/\partial X_i$) are described by:

$$\frac{d\lambda_1}{dt} = -[\lambda_1 + 2\lambda_3(1+\eta)]\, k_1 h^{\frac{1}{2}} \frac{d}{dm}\left[\frac{1-m}{g}\right] - \lambda_3(2+\eta)k_3 \frac{d}{dm}\left[\frac{(1-m)^2}{g^2}\right] \qquad (B\text{-}2)$$

$$\frac{d\lambda_2}{dt} = -[\lambda_1 + 2\lambda_3(1+\eta)]\, k_1 \frac{(1-m)}{g}\frac{d}{dc}(h^{\frac{1}{2}}) - [2a\lambda_1 + \lambda_2 + 2a\eta\lambda_3]\, k_2 \frac{d}{dc}(h) \qquad (B\text{-}3)$$

$$\frac{d\lambda_3}{dt} = 0 \qquad (B\text{-}4)$$

The boundary conditions on the state eqs 7, 8 and 10 and adjoint eqs., B-1 to -4, for the case where polymer is not initially present are:

	$t = 0$	$t = 0$
m =	0	m^*
c =	0	$c^* = \frac{(2-\eta)}{a\bar{X}_n^*} m^*$
ξ_2	0	min
λ_1	----	---
λ_2	----	---
λ_3	----	-1

(B-5)

Therefore, $\lambda_3 = -1$

Along the optimal path, where $H = 0$, the $\partial H/\partial y$ is given by:

$$\frac{\partial H}{\partial y} = (E_2-E_1)(\lambda_1-2-2\eta)k_1 h^{\frac{1}{2}} \frac{(1-m)}{g} + (E_3-E_2)(2+\eta)k_3 \frac{(1-m)^2}{g^2} \qquad \text{(B-6)}$$

From the definition of k_1, k_2 and k_3 the following identities can be proven:

$$k_3 = \frac{k_1^2}{2ak_2}$$
$$(E_2-E_1) = -2(E_3-E_2) \qquad \text{(B-7)}$$

Substitution of (B-7) into (B-6) yields:

$$\frac{\partial H}{\partial y} = (E_2-E_1)(\lambda_1-2-2\eta)k_1 h^{\frac{1}{2}} \frac{(1-m)}{g} - 2(E_2-E_1)\frac{(2+\eta)}{2a} \frac{k_1^2}{k_2} \frac{(1-m)^2}{g^2} \qquad \text{(B-8)}$$

Along the stationary policy, $y^* \leq y \leq y_*$, $\partial H/\partial y = 0$:

$$\frac{\partial^2 H}{\partial y^2} = -(E_2-E_1)^2 \frac{(2+\eta)}{2a} \frac{k_1^2}{k_2} \frac{(1-m)^2}{g^2} < 0 \qquad \text{(B-9)}$$

Therefore, the stationary policy can form part of the optimal path.

Applying the criteria for the optimal path, eq. 16, to and rearranging B-8 yields:

$$\frac{k_1(1-m)}{ak_2h^{\frac{1}{2}}g} \gtreqless \frac{1}{(2+\eta)} \quad (\lambda_1 - 2 - 2\eta) \quad ; \quad \begin{matrix} y = y_* \\ y = y_s \\ y = y^* \end{matrix} \tag{B-10}$$

Substitution of eq. 13 into B-10 yields:

$$\bar{X}_{n,i} \gtreqless \frac{(\lambda_1 - 2 - 2\eta)}{(2+\eta)(2-\eta)} + \frac{2}{(2-\eta)} \quad ; \quad \begin{matrix} y = y_* \\ y = y_s \\ y = y^* \end{matrix} \tag{B-11}$$

But along the stationary path, $\partial H/\partial y = 0$. Substituting eq. B-10 into B-2 yields:

$$\frac{d\lambda_1}{dt} = -[\lambda_1 - 2 - 2\eta]\, k_1 h^{\frac{1}{2}} \frac{d}{dm}\left(\frac{1-m}{g}\right)$$

$$\frac{-(E_2-E_1)}{2(E_2-E_1)} (\lambda_1 - 2 - 2\eta)\, k_1 \frac{h^{\frac{1}{2}}}{\frac{(1-m)}{g}} \left[2\frac{(1-m)}{g}\right] \frac{d}{dm}\left(\frac{1-m}{g}\right)$$

$$\frac{d\lambda_1}{dt} = 0 \; ; \quad \lambda_1 = \text{const.} \tag{B-12}$$

And therefore along y_s

$$\bar{X}_{n,i} = \text{const.} \tag{B-13}$$

as predicted by Hoffman, et al. [6].

APPENDIX C. DERIVATION OF CRITERIA FOR MAXIMUM D_n POLICY

The state of the system is described by eqs. 7, 8 and 10. The Hamiltonian is given by eq. B-1, and the adjoint variables are described by eqs. B-2 to B-4. The boundary conditions for the state and adjoint variables with the exception of λ_3 are given by B-5. The boundary conditions for λ_3 are:

	$t = 0$	$t = 0$
λ_3	---	+1

(C-1)

Therefore, $\lambda_3 = +1$.

Along the optimal path where $H = 0$:

$$\frac{\partial H}{\partial y} = (E_2-E_1)(\lambda_1 + 2 + 2\eta)k_1h^{\frac{1}{2}} \frac{(1-m)}{g} + 2(E_2-E_1)\frac{(2+\eta)}{2a}\frac{k_1^2}{k_2}\frac{(1-m)^2}{g^2} \tag{C-2}$$

Along the stationary policy, $y^* \leq y_s \leq y_*$, $\partial H/\partial y = 0$:

$$\frac{\partial^2 H}{\partial y^2} = (E_2 - E_1)^2 \quad \frac{(2+\eta)}{2a} \quad \frac{k_1^2}{k_2} \quad \frac{(1-m)^2}{g^2} > 0 \qquad \text{(C-3)}$$

Therefore, the stationary policy minimizes rather than maximizes the Hamiltonian, and, from the Maximum Principle, cannot form part of the optimal path.

Rearrangement of C-2 and the application of eqs. 3, 6 and C-3 yields the criteria for the optimal policy:

$$X_{n,i} \begin{matrix} < \\ > \end{matrix} \frac{-(\lambda_1 + 2 + 2\eta)}{(2+\eta)(2-\eta)} + \frac{2}{(2-\eta)} \quad ; \quad \begin{matrix} y = y^* \\ y = y_* \end{matrix} \qquad \text{(C-4)}$$

Captions

Table I	Kinetic Data
Table II	Summary, Examples of Minimum and Maximum Dispersion Indicies
Table III	Summary of Experimental Results
Figure 1	Map of $\bar{X}_{n,i}$ Behavior
Figure 2	Temperature Policies and Chain Lengths-Example 1
Figure 3	Temperature Policies and Chain Lengths-Example 2
Figure 4	Temperature Policies and Chain Lengths-Example 3
Figure 5	Molecular Weight Distributions-Example 2
Figure 6	Maximum D_n Policies
Figure 7	Normalized Chromatograms
Figure 8	Temperature Profiles in Idealized Batch Reactor
Figure 9	Molecular Weight Distributions, Comparison of Worst Batch Reactor to Optimal Policies

Table I

KINETIC DATA

	Styrene	Methyl methacylate
A_p, $l.sec.^{-1}mol^{-1}$	1.051×10^7	5.1×10^6
A_t, $l.sec^{-1}mol^{-1}$	1.255×10^9	7.8×10^8
A_d, sec^{-1}	1.58×10^{15}	1.58×10^{15}
E_p, $cal.\ mol.^{-1}$	7060	6300
E_t, $cal.\ mol.^{-1}$	1680	2800
E_d, $cal.\ mol.^{-1}$	30800	30800
$g = (k_t/k_{to})^{\frac{1}{2}}$	$1.0 \quad 0 \leq m \leq .3$ $1.522 - 1.818m \quad .3 \leq m \leq .8$	$1. \quad 0 \leq m \leq .15$ $1./(1. - 28.72m + 228.2m^2 - 239.9m^3) \quad .15 \leq m \leq .6$
η, k_{tc}/k_t	1.0	0.0
f	0.5	0.6
$h(1-c)$	$(1-c)$	$(1-c)$

Table II

SUMMARY, EXAMPLES OF MINIMUM AND MAXIMUM DISPERSION INDICIES

Ex. No.	Polymer	I_o m/l	M_o m/l	T_* °C	T^* °C	k_2/k_1	Conversion Mon	Conversion Init.	$\bar{X}_n$	Gel Eff	Max D_n	Min D_n	Isothermal T, °C	Isothermal D_n	Step Rise D_n	SCSTR D_n
1	Styrene	0.116	8.7	40	120	0.8	0.5	0.25	300	Yes	3.91	1.50	63.8	1.50	3.72	1.7
1A		0.116				0.7		0.25		No	3.57	1.50	61.1	1.53	3.57	1.6
2		0.0323				3.9		0.90		Yes	12.63	1.50	90.0	1.61	5.55	---
2A		0.0323				3.6		0.90		No	9.10	1.50	86.8	1.52	6.02	---
3		0.133				1.4	0.3	0.26	150	Yes	6.51	1.49	81.5	1.50	6.51	---
3A		0.133				1.4	0.3	0.26	150	No	6.51	1.49	81.5	1.50	6.51	---
4	MMA	0.00725				1.8	0.5	0.25	2000	Yes	36.2	2.01	87.6	3.96	4.44	4.0
4A		0.00725				0.7		0.25		No	6.64	2.00	65.5	2.05	6.64	2.1
5		0.00242				6.4		0.75		Yes	103.0	3.32	107.5	5.05	5.88	---
5A		0.00242				2.5		0.75		No	11.5	2.00	82.9	2.00	10.9	---

Table III

SUMMARY OF EXPERIMENTAL RESULTS

Run No	Initial Temp °C	Final Temp °C	M_o Mol/l	I_o mole/l	Time sec	Time To switch sec	EXPERIMENTAL Conv	Xw	Xn	Dn	CALCULATED Conv	Xw	Xn	Dn
								2800	700	3.6		2480*	1310*	1.87
NBS-706														
1	60	60	8.37	0.13	3720	------	0.104	650	190	3.5	0.099	524	350	1.5
2	60	60	8.37	0.13	23,160	------	0.605	620	270	2.3	0.505	476	317	1.5
3	40	40	8.53	0.14	30,300	------	0.11	1600	630	2.5	0.102	1273	849	1.5
4	40	40	8.53	0.14	268,080	------	0.8	3300	1200	2.7	0.891	1592	904	1.77
5	87.2	87.2	8.13	0.0110	4920	------	0.3	1200	590	2.0	0.277	787	516	1.52
6	100	40	8.02	0.0108	259,920	480	0.312	2500	570	4.4	0.254	3481	667	5.22
7	80.8	80.8	8.19	0.126	2326	------	0.315	400	230	1.7	0.337	224	150	1.5
8	40	100	8.53	0.131	63,660	63,440	0.37	1400	180	7.8	0.335	773	151	5.12

*Given by National Bureau of Standards for NBS-706

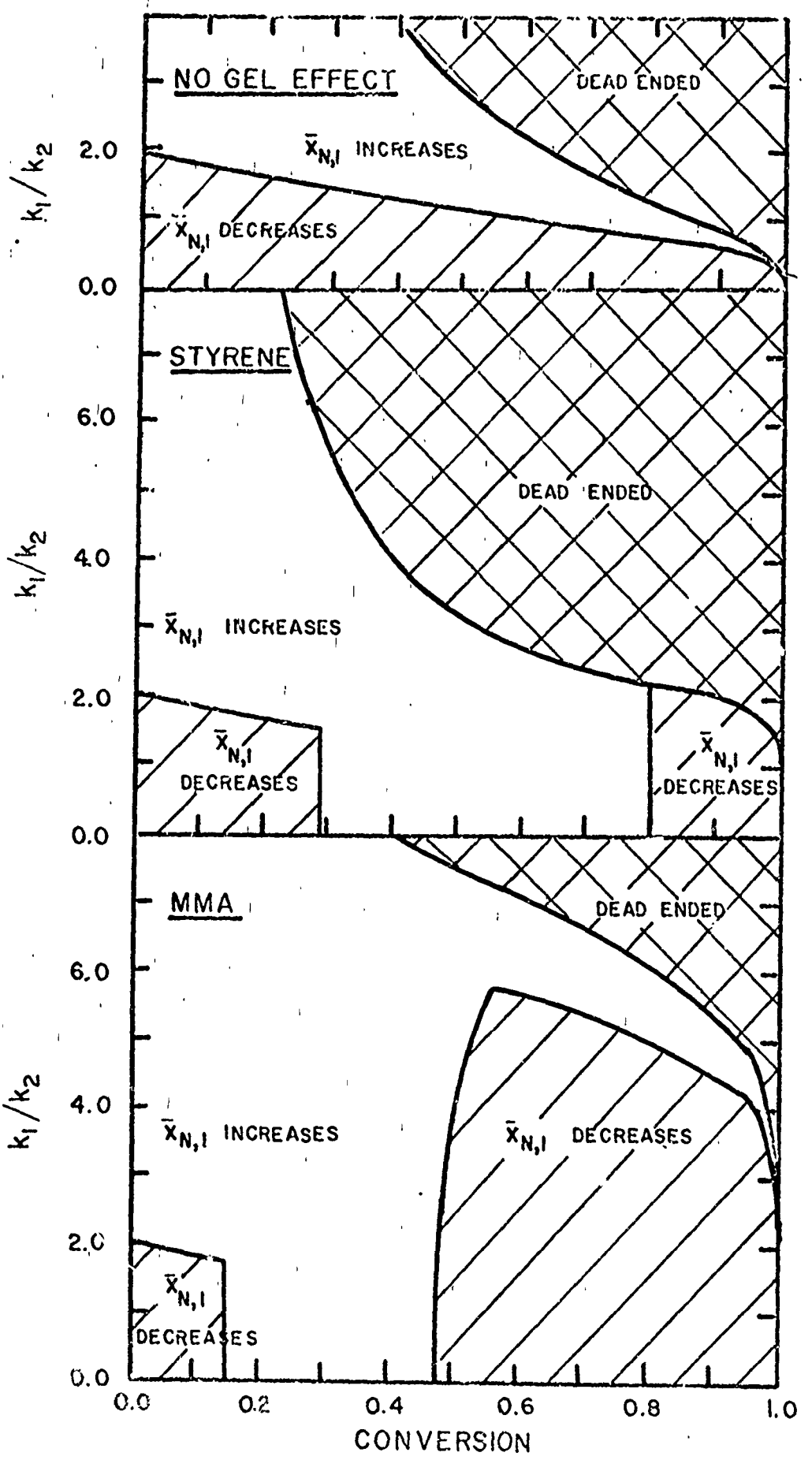
NO GEL EFFECT
DEAD ENDED
$\bar{X}_{N,I}$ INCREASES
$\bar{X}_{N,I}$ DECREASES
STYRENE
DEAD ENDED
$\bar{X}_{N,I}$ INCREASES
$\bar{X}_{N,I}$ DECREASES
$\bar{X}_{N,I}$ DECREASES
MMA
DEAD ENDED
$\bar{X}_{N,I}$ INCREASES
$\bar{X}_{N,I}$ DECREASES
$\bar{X}_{N,I}$ DECREASES
k_1/k_2
2.0
0.0
6.0
4.0
2.0
0.0
6.0
4.0
2.0
0.0
0.0
0.2
0.4
0.6
0.8
1.0
CONVERSION

Figure 1.

Figure 2

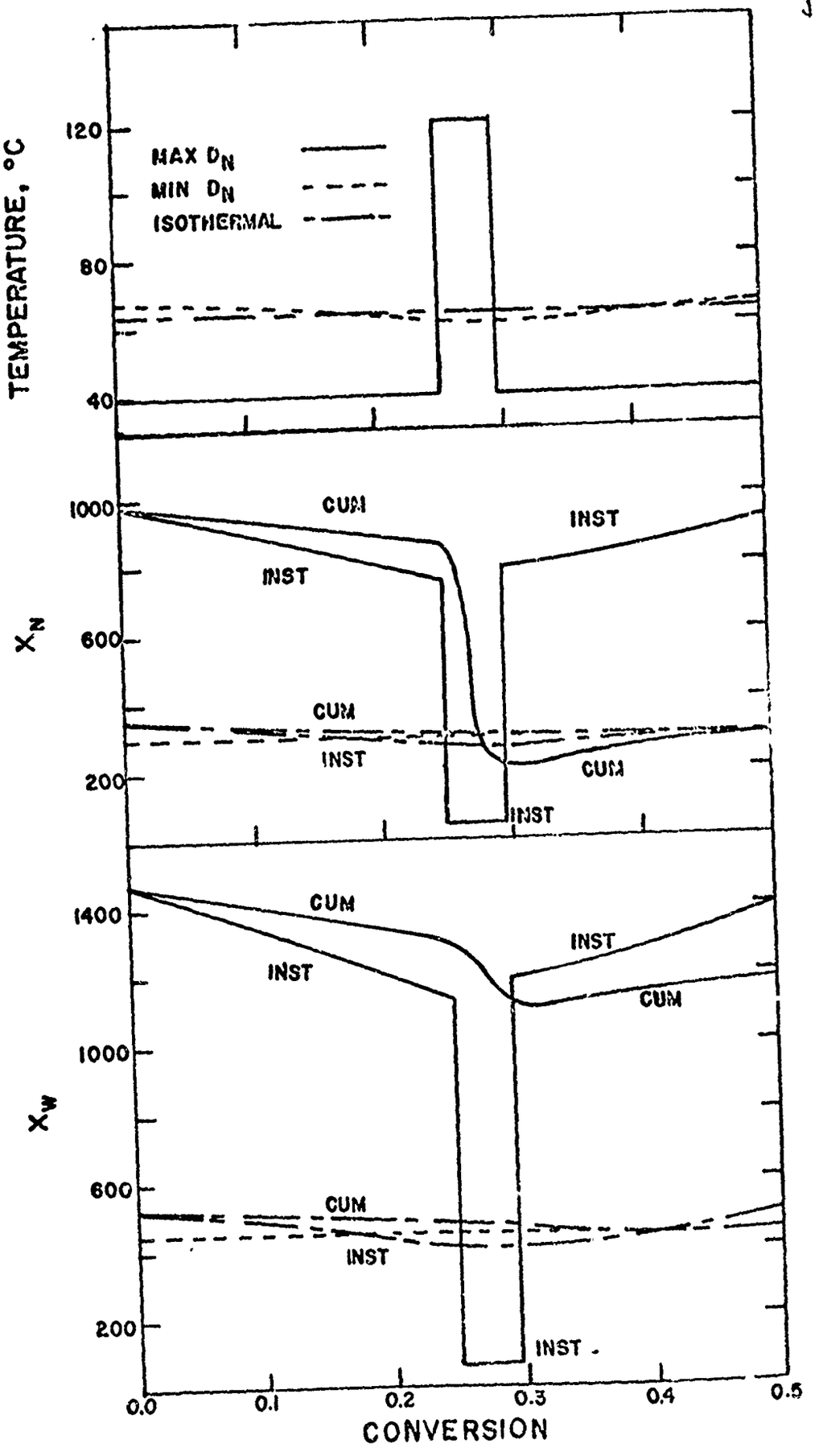
TEMPERATURE, °C
120
80
40
MAX D_N
MIN D_N
ISOTHERMAL
X_N
1000
600
200
CUM
INST
INST
CUM
CUM
INST
INST
X_W
1400
1000
600
200
CUM
INST
INST
CUM
CUM
INST
INST
0.0
0.1
0.2
0.3
0.4
0.5
CONVERSION

Figure 3

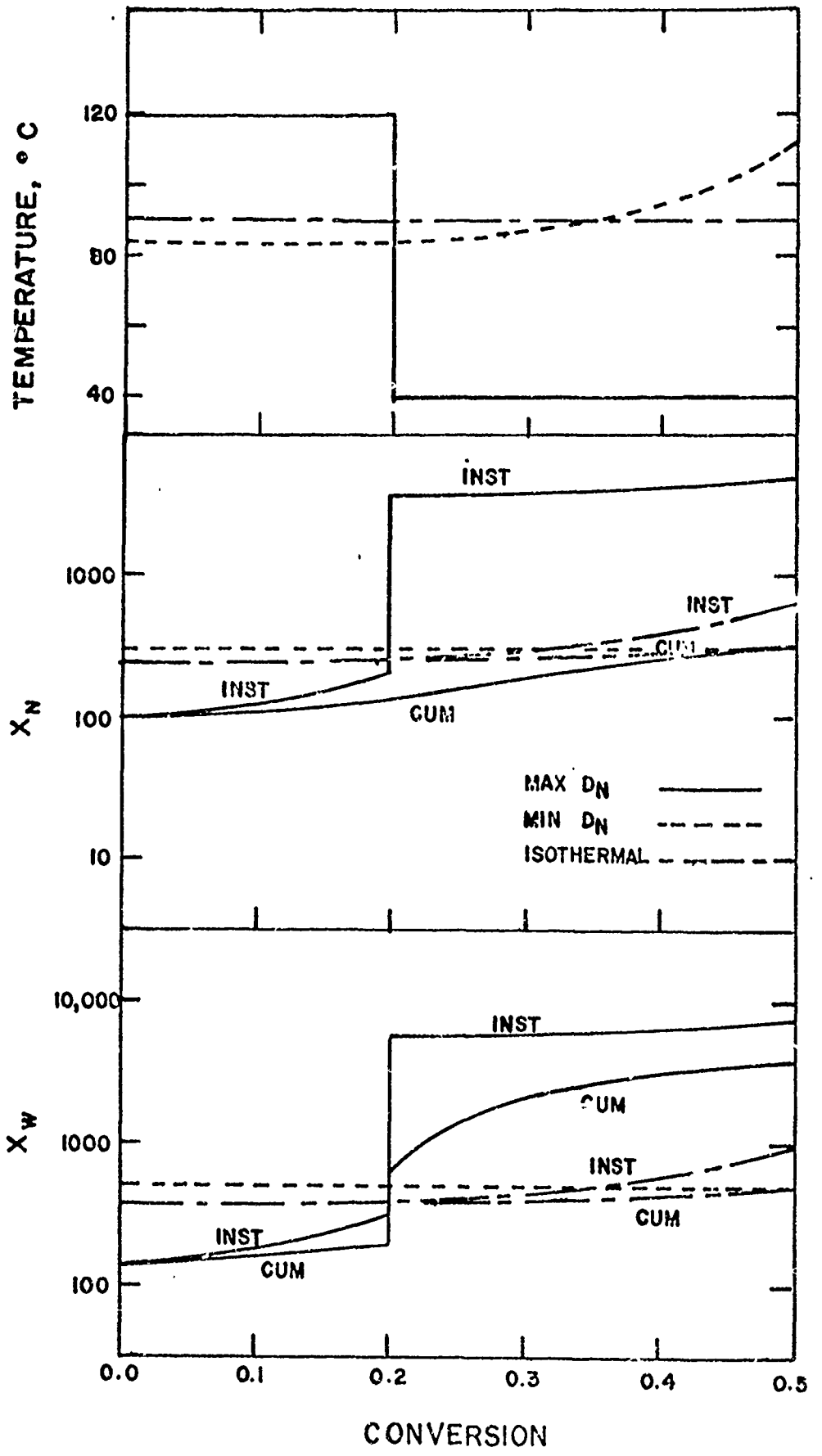
TEMPERATURE, °C
120
80
40
INST
1000
INST
CUM
INST
CUM
X_N
100
MAX D_N
MIN D_N
ISOTHERMAL
10
10,000
INST
CUM
1000
INST
CUM
INST
CUM
X_W
100
0.0
0.1
0.2
0.3
0.4
0.5
CONVERSION

Figure 4

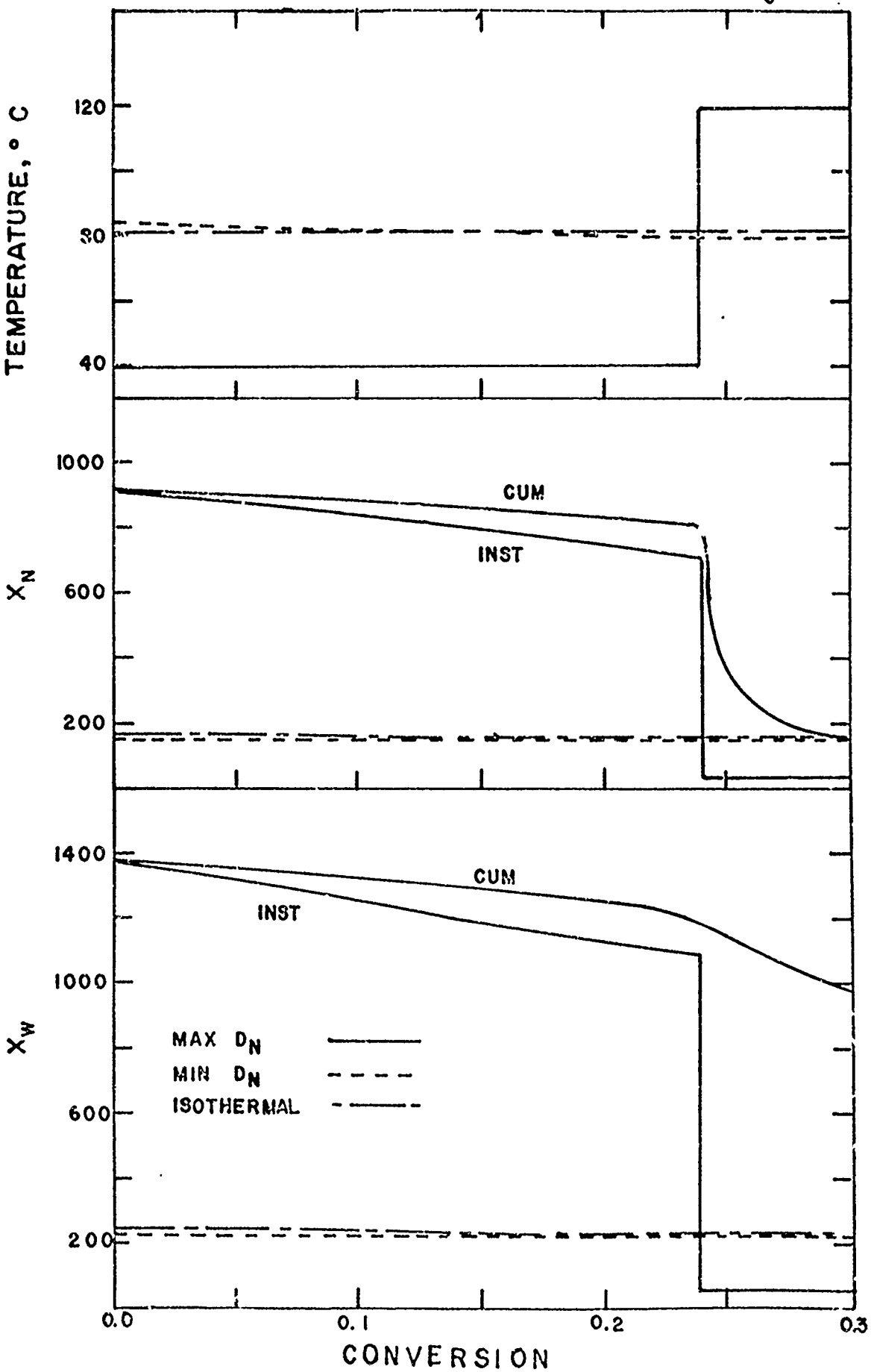
TEMPERATURE, ° C
120
80
40
X_N
1000
600
200
CUM
INST
X_W
1400
1000
600
200
CUM
INST
MAX D_N
MIN D_N
ISOTHERMAL
0.0
0.1
0.2
0.3
CONVERSION

Figure 5

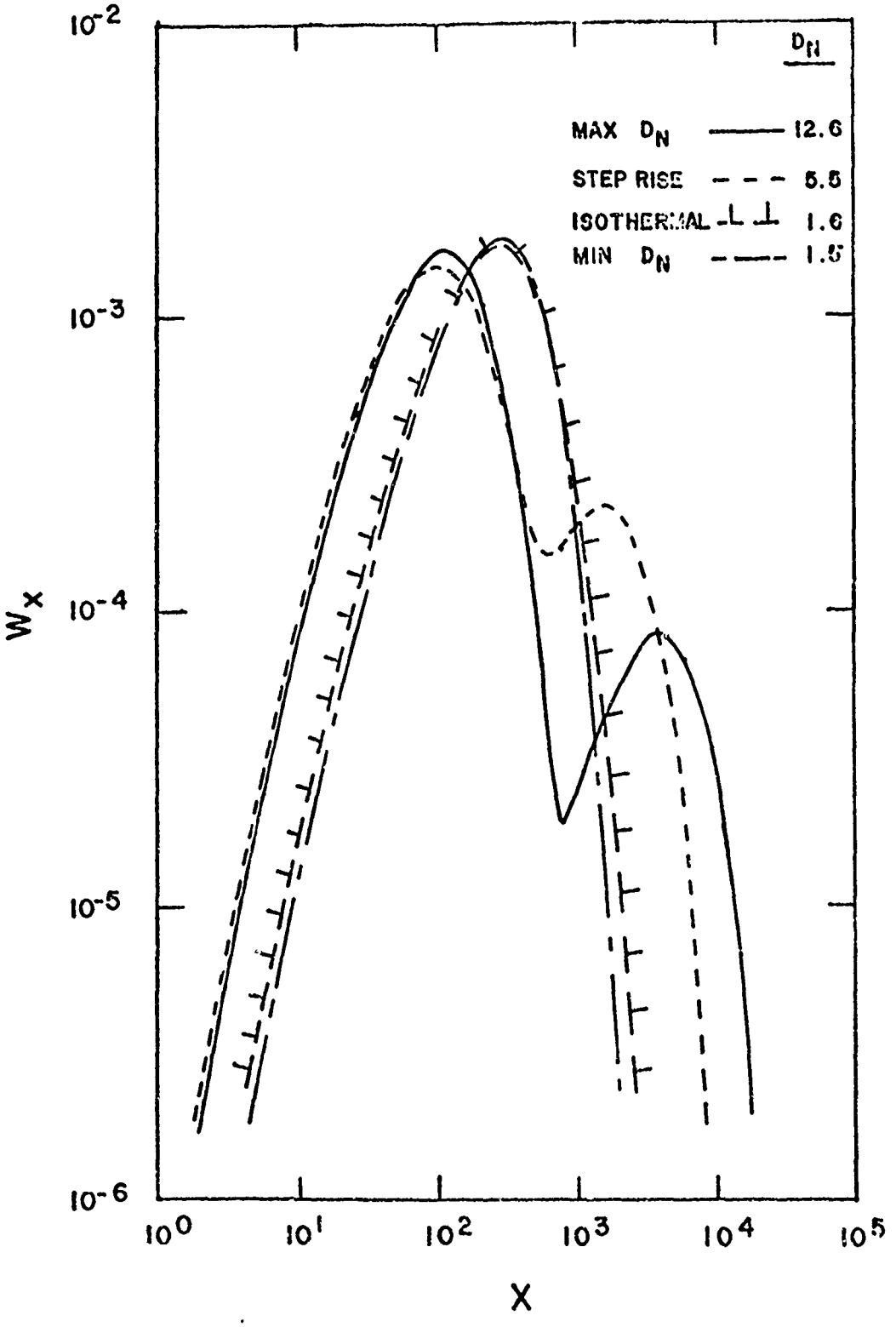
10^{-2}
10^{-3}
10^{-4}
10^{-5}
10^{-6}
W_X
10^0
10^1
10^2
10^3
10^4
10^5
X
D_N
MAX D_N —— 12.6
STEP RISE - - - 5.5
ISOTHERMAL ⊥⊥ 1.6
MIN D_N - —— 1.5

Figure 6

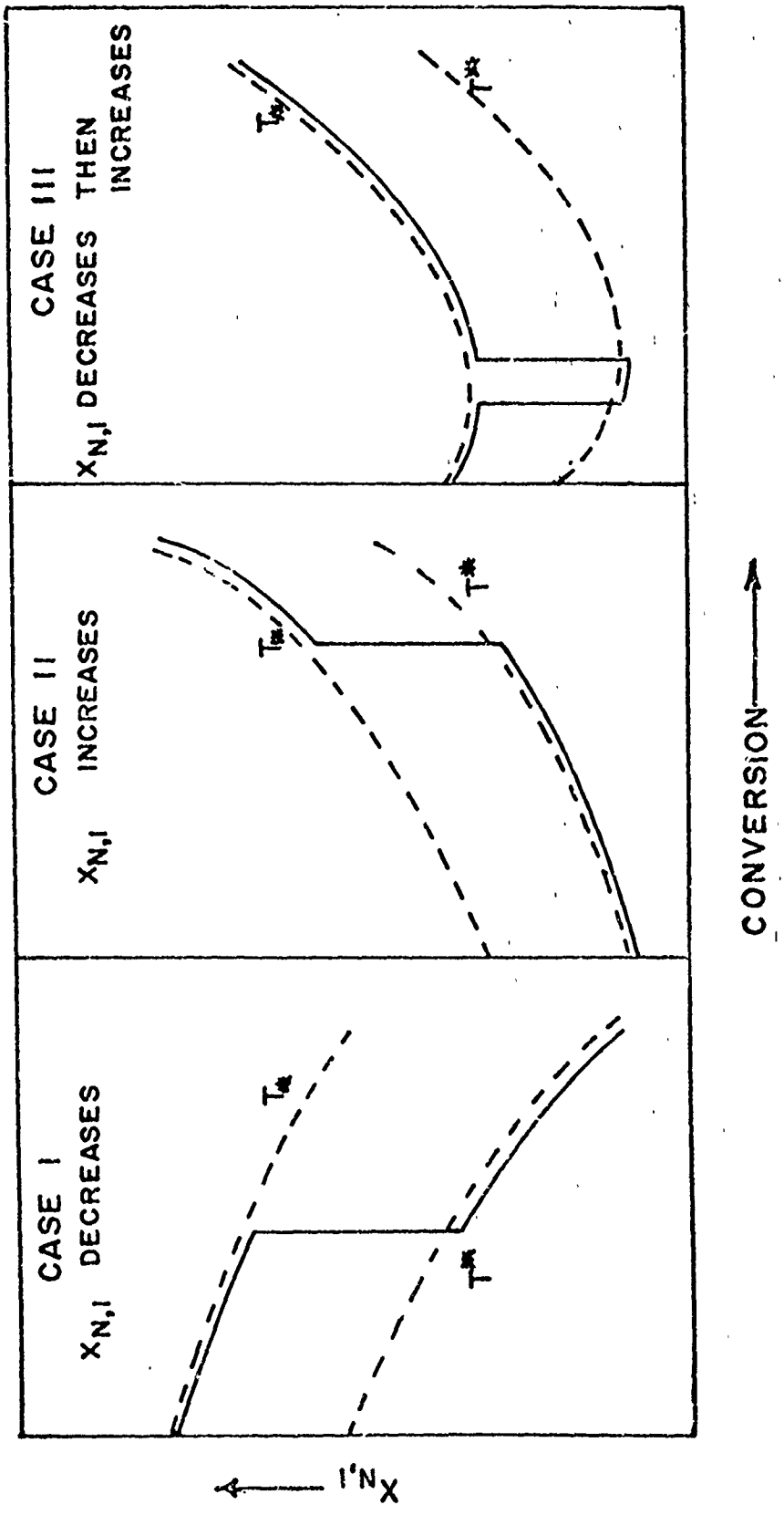
CASE III
$X_{N,I}$ DECREASES THEN INCREASES
CASE II
$X_{N,I}$ INCREASES
CASE I
$X_{N,I}$ DECREASES
T^*
T^{**}
T^{**}
T^*
T^*
T^{**}
CONVERSION
$1/N_X$

Figure 7

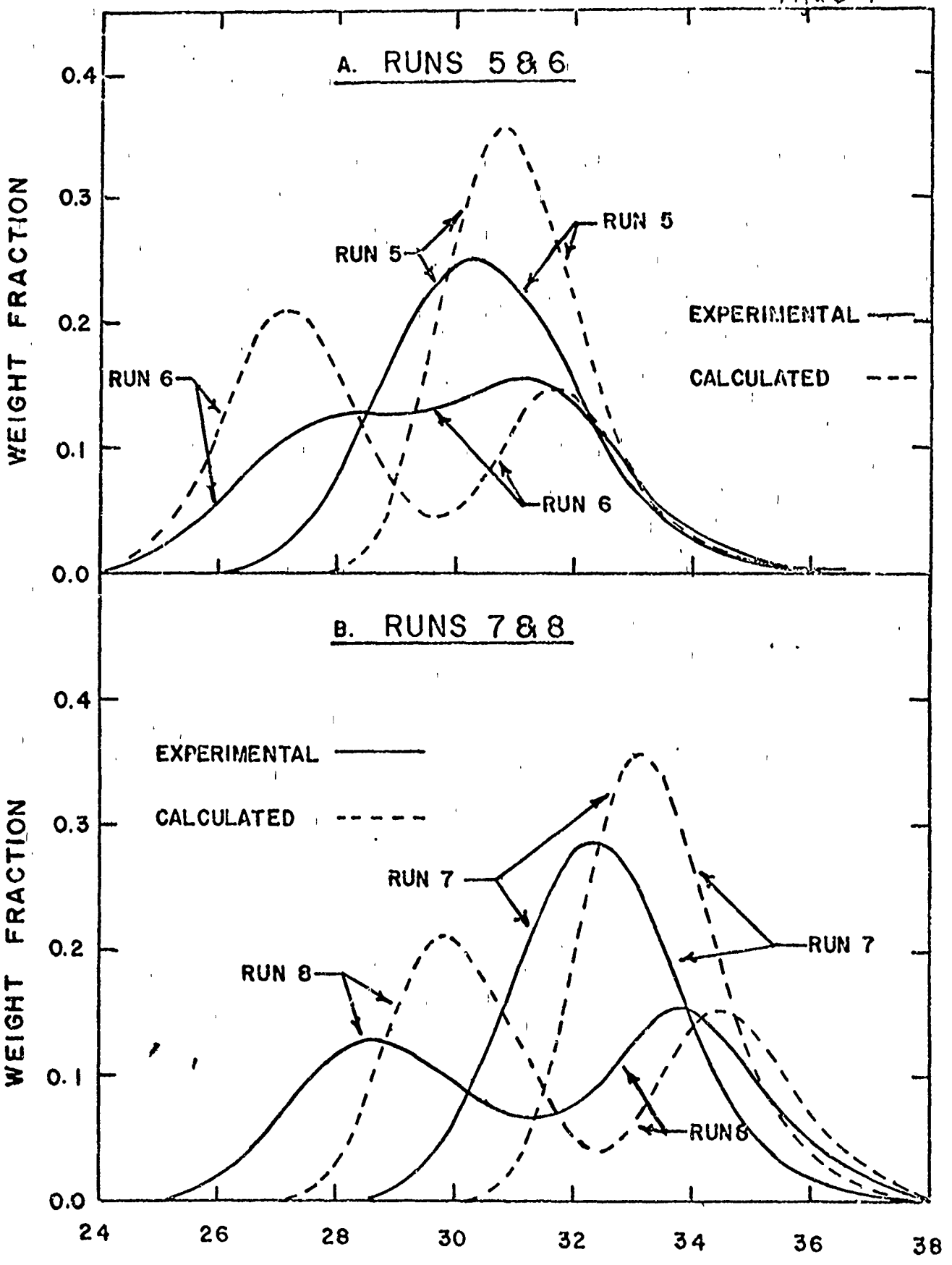
A. RUNS 5&6
RUN 5
RUN 5
RUN 6
RUN 6
EXPERIMENTAL
CALCULATED
WEIGHT FRACTION
0.0
0.1
0.2
0.3
0.4
B. RUNS 7&8
EXPERIMENTAL
CALCULATED
RUN 7
RUN 7
RUN 8
RUN 8
WEIGHT FRACTION
0.0
0.1
0.2
0.3
0.4
24
26
28
30
32
34
36
38
ELUTION VOLUME, COUNTS (1 COUNT = 5 ML)

Figure 8

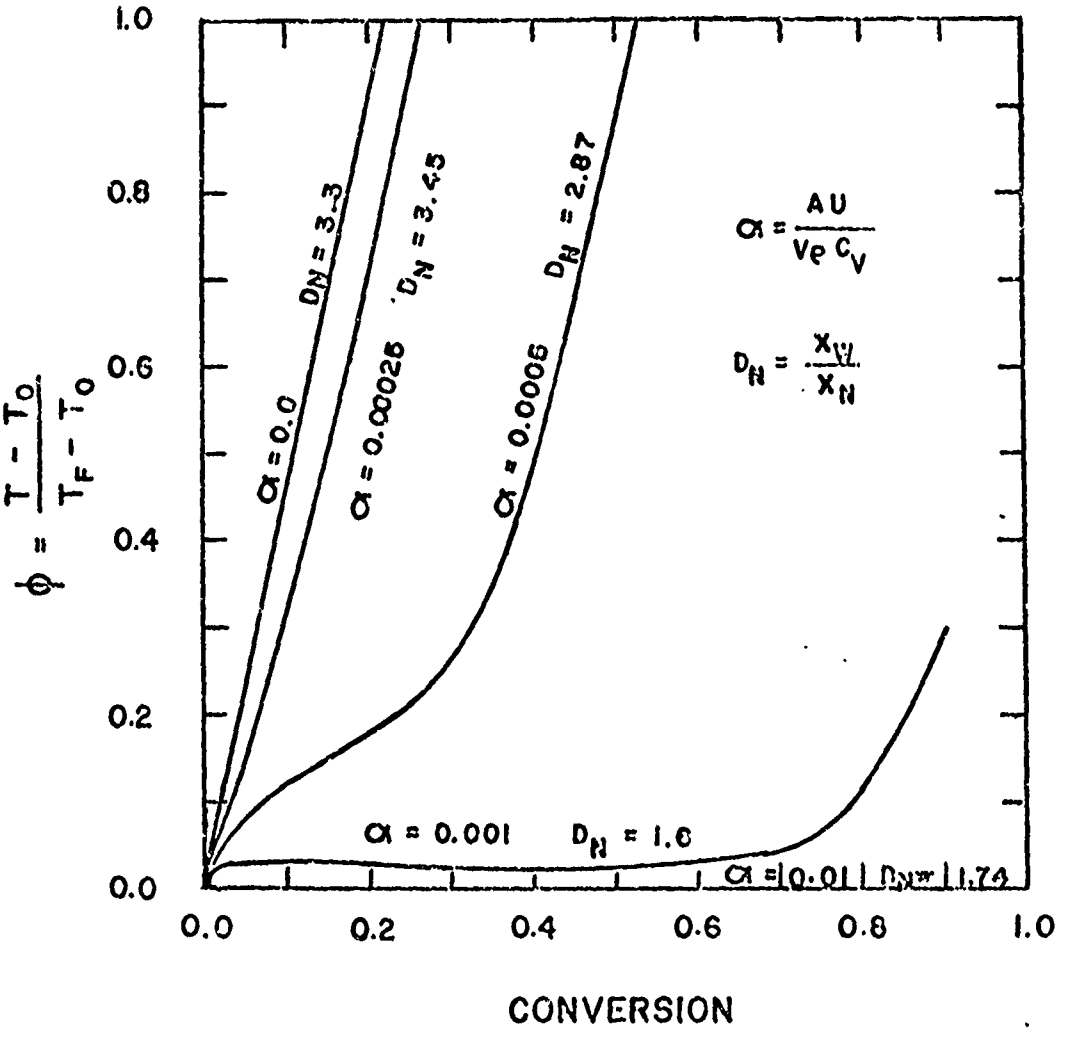
1.0
0.8
0.6
0.4
0.2
0.0
0.0
0.2
0.4
0.6
0.8
1.0
$\phi = \frac{T - T_0}{T_F - T_0}$
CONVERSION
$\alpha = \frac{AU}{V\rho C_V}$
$D_N = \frac{X_W}{X_N}$
$\alpha = 0.0$ $D_N = 3.3$
$\alpha = 0.00028$ $D_N = 3.45$
$\alpha = 0.0006$ $D_N = 2.87$
$\alpha = 0.001$ $D_N = 1.6$
$\alpha = 0.01$ $D_N = 1.74$

Figure 9

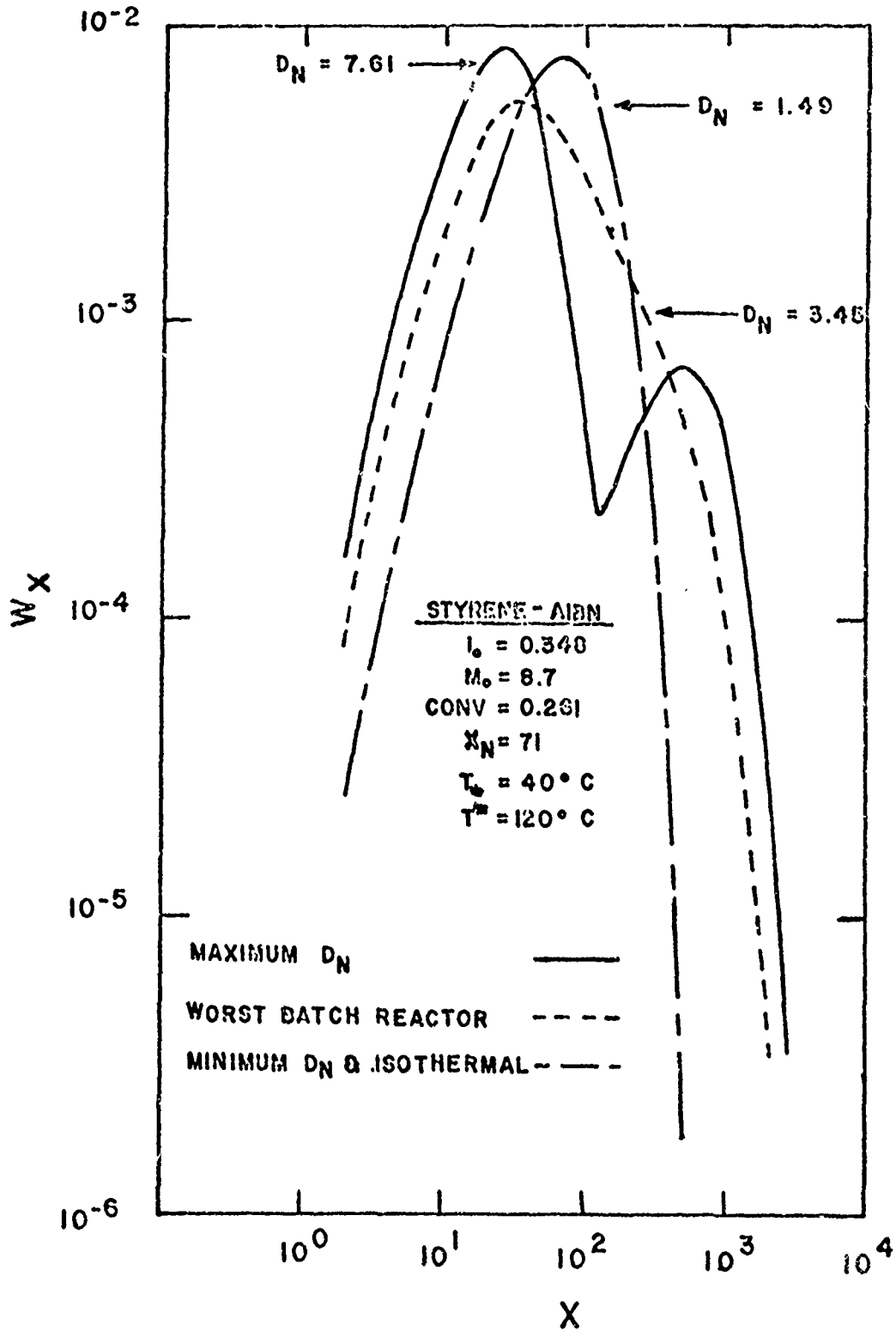
10^{-2}
10^{-3}
10^{-4}
10^{-5}
10^{-6}
W_X
D_N = 7.61
D_N = 1.49
D_N = 3.46
STYRENE - AIBN
I_o = 0.340
M_o = 8.7
CONV = 0.261
X_N = 71
T_o = 40° C
T^{max} = 120° C
MAXIMUM D_N
WORST BATCH REACTOR
MINIMUM D_N & ISOTHERMAL
10^0
10^1
10^2
10^3
10^4
X